DYNAMIC RESPONSE OPTIMIZATION USING MSC/NASTRAN

M. Chargin and H. Miura
NASA Ames Research Center, Moffett Field, California

G. Clifford
Cray Research Inc., Mendota Heights, Minnesota

ABSTRACT

Numerical optimization techniques are used to modify the dynamic response at a specified point(s) of a structure due to a steady state narrow band excitation. Calculation of steady state vibration amplitude is reduced to the solution of linear equations with complex coefficients. The sensitivity of the dynamic amplitudes with respect to the structural parameter perturbations can be computed with the same technique as the one used in the static displacement sensitivity without requiring eigenvector sensitivity. Approximate models for critical structural responses are created based on the sensitivity data to reduce the amount of computational effort and to enable the design of structures of practical scale and complexity. This approach is general in that it accommodates static, dynamic, and frequency constraints simultaneously as long as their computational models are available. It can be used in optimizing mass distribution as well as stiffness modifications of practical structures.

Two example problems are solved to demonstrate the capability of these techniques. One is a simply supported beam subjected to a rotating force and static gravity load. The other example is an engine support structure which possesses significant size and complexity. It is also loaded by static gravity loads and forces due to rotating mass unbalance.

INTRODUCTION

This paper describes an automated design technique for modifying structural models. The technique provides design engineers with a method of designing or modifying a structure to achieve given objectives. Specifically, modifications of a structure, excited by harmonic loads of constant frequency, are considered with the intent of reducing steady state vibration amplitudes.

Finite element analyses of linear structural models provide structural dynamicists with a wealth of information regarding the expected behaviors of the structure under the dynamic loads. Usually, information such as natural

vibration frequencies, mode shapes, modal damping coefficients, modal participation factors, and amplification factors is studied and interpreted for engineering significance by structural dynamicists. However, additional data are required for automated design of new structures or modification of existing designs.

First, it is necessary to identify the parts of the structure that should be modified to effectively reduce the dynamic response. Subsequently, a determination must be made regarding the size of the changes to be made to achieve the desirable dynamic characteristics without adversely affecting other factors, such as weight and static strength/stiffness requirements.

The first task is the sensitivity analysis of structural responses with respect to structural design variables, and identification of candidate members that have strong influence on dynamic behavior. This has been studied extensively in the past. Studies include Vincent circle (conformal mapping) method (Done[1]; Done[2]; Done[3]; Hanson[4]), forced response strain energy method (Hanson[4]; Hanson[5]; Sciarra[6]), matrix perturbation method (King[7]; Wang[8]) and analytic differentiation method (Kitis[9]).

The second issue is the modification of structural design based on the sensitivity data. The modifications of the design become critically important because they must address the finite changes and nonlinearities of the responses with respect to the design variables. Most of the works cited above include some effort to modify the identified structural parts to reduce vibratory responses. For example, Kitis et al.[9] used the sensitivity data obtained by a matrix perturbation method to demonstrate its applicability to absorber design as well as structural stiffness modifications. Bartlett[10] presented an excellent study on the applicability of conformal mapping technique to absorber design using both the test data and the results obtained from mathematical models.

The design techniques proposed in these previous studies addressed solution methods for specific problems and they may not be readily incorporated for cases in which many different design conditions and design parameters are considered at the same time. However, structural optimization techniques described in this paper allow generic integration of different disciplines including dynamic and static design requirements. The use of mathematical programming as the design decision tool is not new, because Wang[8] and Kitis[9] presented the basic idea and demonstrated its feasibility. However, it was shown in the history of structural optimization, Schmit et al[11], that a simple combination of these two capabilities fails to produce a practical synthesis capability due to excessive data processing effort. The key to overcoming this difficulty is the use of approximation concepts described in a previous paper. A reasonable number of system analyses required by nonlinear programming algorithms are at least several times the number of design variables, if sensitivity analyses are formed by finite difference. For example, if 20 structural parameters are allowed to change simultaneously, the number of system analyses needed for convergence will be at least 50 to 100. When sensitivity analyses are performed by the implicit differentiation technique, the number of analyses decreases significantly, but it will be difficult to have less than 20 even for relatively well-behaved problems using the best available optimization algorithms. Therefore, it is essential to sever direct communication between structural analysis and optimization.

This is done by creating an approximate mathematical model of the "exact" finite element model to act as a buffer between these two tasks. The simplest form of the approximation is the first order Taylor series expansion, which can be created readily once the sensitivity data are available. Collection of the Taylor series expansions of only the critical and potentially critical system responses, while temporarily discarding others, constitutes an approximate representation of the original finite element model. Taylor series expansions are easy to evaluate, thus optimization with respect to the approximate models becomes a trivial task. Efficiency of optimization algorithms in terms of the number of function evaluations is no longer important. The CPU time required for one optimization with approximate models is often less than 1% of one finite element analysis, so it is possible to run it interactively on minicomputers. In practice, several optimization runs are often executed based on the same approximate models by changing control parameters allowables or even modifying objective functions to see the effects on design modifications.

The approximate models are not limited to simple linearization of nonlinear functions, but are always explicit functions of design variables and easy to evaluate, as described in Schmit et al[11] and later in this paper. Since the approximate models are valid only in the neighborhood of the current design point, it is dangerous to make large design changes based on the approximate model. The degree of this danger depends on the nonlinearity of system responses. Usually, artificial move limits are imposed on each design variable to restrict the magnitude of the design changes, based on the current set of approximate models. For this reason it is necessary to repeat a sequence of procedures composed of:

1. Complete structural analysis by finite element analysis.
2. Identification of critical and potentially critical structural responses.
3. Evaluation of sensitivities of identified response.
4. Construction of approximate mathematical models.
5. Optimization with respect to the approximate models.

This sequence is referred to as one iteration of design optimization. The number of finite element analyses is equal to the number of iterations plus one, since it is desirable to analyze the final design generated in the last iteration. Obviously, it is important to reduce the number of iterations. This can be achieved by allowing large changes in the design variables in each design iteration. However, if the design change made in one iteration exceeds the range within which approximate models are valid, the overall design procedure may not converge. Consequently, it is important to select approximate models that are valid for large design variable changes and to work within the limits in each design iteration.

The computer program used in this study was originally implemented to support an in-house composite wing design project. It takes advantage of the sensitivity analysis capability installed in MSC/NASTRAN. Currently, MSC/NASTRAN does not support sensitivity analysis for frequency responses, so a new DMAP program was written to add this capability. Application of this system to a large scale static problem was already reported in literature,Vanderplaats et al[12]. The optimizer used was the well-known CONMIN[13] program, which could be replaced by any reliable constrained

function minimization code. The new contributions of this paper may be summarized as follows:

1. Structural optimization capability that can consider static responses (stress, strain and deformation), natural frequencies, and steady state dynamic responses.
2. Incorporation of approximation concepts for all structural responses to achieve adequate efficiency in solving large scale problems.
3. Error analysis of approximate representations of frequency responses near resonance frequency.
4. Applications of structural synthesis capabilities to difficult design problems involving dynamic responses.

However, two important problems associated with structural optimization involving dynamic requirements are not addressed in this paper. The first problem is the strong nonlinearity of the dynamic response near resonance. A proposed approach described in Appendix A may help to alleviate this problem, but it will require extensive testing. The second problem is a disjoint feasible design space pointed out previously (Johnson et al[14] and Mills-Curran et al[15]). For lightly damped structures, dynamic responses are large near the resonance, so design modifications that cause one or more natural frequencies to approach the forcing frequency are not permissible. If the initial design has the forcing frequency, Ω, between w_i and $w_{(i+1)}$, the design must be confined in the subspace to keep the forcing frequency between w_i and $w_{(i+1)}$. If the initial design is selected to have the forcing frequency between $w_{(i-1)}$ and w_i, then the design will remain in the different subspace. Since there is no information as to which subspace will yield the best design, and since there is no current mechanism to jump from one subspace to the other, the final design is dictated by the choice of the initial design. Using optimization, the design will likely be improved within a particular subspace, but there may be better subspaces elsewhere.

DIRECT FREQUENCY RESPONSE ANALYSIS AND STRUCTURAL OPTIMIZATION PROBLEMS

The equilibrium equation of a linear structural system considered herein may be written as:

$$[\mathbf{M}]\ddot{\mathbf{U}}(t) + [\mathbf{C}]\dot{\mathbf{U}}(t) + (1+ig)[\mathbf{K}]\mathbf{U}(t) = \mathbf{F}(t) \qquad (1)$$

where g is the structural damping factor, **K** is the stiffness matrix, **C** is the viscous damping matrix, **M** is the mass matrix, **F**(t) is the external force vector, and **U**(t) is the displacement vector. For static loadings, Eq. (1) is reduced to:

$$[\mathbf{K}]\mathbf{U}_s = \mathbf{F}_s \qquad (2)$$

where $\mathbf{F}_s$ is the static load vector and $\mathbf{U}_s$ is the static displacement vector.

The steady state dynamic response of a linear structural system subject to an excitation with a constant frequency, Ω, is formulated by considering the

forcing function $\mathbf{F}(t)$ to be equal to $(\mathbf{F}_R+i\mathbf{F}_I)e^{i\Omega t}$, and the steady state solution $(\mathbf{U}_R+i\,\mathbf{U}_I)e^{i\Omega t}$ can be computed by solving the linear equation with complex coefficients as:

$$\{\mathbf{A}\}\ \{\mathbf{U}_R+i\mathbf{U}_I\} = \{\mathbf{F}_R+i\mathbf{F}_I\} \tag{3}$$

where

$$\{\mathbf{A}\} = \{-\Omega^2[\mathbf{M}] + i\Omega[\mathbf{C}] +(1+ig)[\mathbf{K}]\}$$

Even if the response considered here is dynamic, it is not necessary to carry out expensive eigenvalue analysis. The advantages of this approach when compared to the modal reduction techniques are significant when the response sensitivity analysis is considered. Sensitivity of the dynamic response vector $[\mathbf{U}_R+i\mathbf{U}_I]$ with respect to the i-th design variable x_i can be computed as the solution of the following linear equation (8)

$$\mathbf{A}\frac{\partial(\mathbf{U}_R+i\mathbf{U}_I)}{\partial x_i} = \frac{\partial(\mathbf{F}_R+i\mathbf{F}_I)}{\partial x_i} - \frac{\partial \mathbf{A}}{\partial x_i}(\mathbf{U}R+i\mathbf{U}I) \tag{4}$$

If the magnitude of the j-th degree of freedom u_j is used in the formulation of the design problem, u_j can be computed as:

$$u_j = (u_{Rj}^2 + u_{Ij}^2)^{1/2} \tag{5}$$

The sensitivity of the magnitude u_j can be computed by differentiating Eq. (5) with respect to x_i:

$$\frac{\partial u_j}{\partial x_i} = \frac{1.0}{u_j}\left(uRj\ \frac{\partial u_R}{\partial x_j} + uIj\ \frac{\partial u_I}{\partial x_j}\right) \tag{6}$$

Currently, MSC/NASTRAN does not support sensitivity analysis of direct frequency responses, but it is possible to assemble Eq. (4) by a DMAP program, since stiffness and mass matrix sensitivities are available in the static sensitivity analysis module. Eq. (4) can be solved within MSC/NASTRAN by a built-in linear equation solver for complex matrices. Since MSC/NASTRAN supports sensitivities of static responses and natural vibration frequencies, it is possible to integrate these capabilities to build a unique structural synthesis program that can solve practical design problems, considering both static and dynamic problems simultaneously. The design problems are formulated into a standard mathematical programming problem in the form as:

$$\begin{aligned} &\text{Minimize} \quad \mathbf{OBJ}(\mathbf{x}) \\ &\text{Subject to:} \quad \mathbf{G}_j(\mathbf{x}) \le 0 \quad j = 1,2,\ldots J \end{aligned} \tag{7}$$

where $\mathbf{OBJ}(\mathbf{x})$ is a scalar function of design variables $\mathbf{x} = (x_1,x_2,\ldots,x_n)$ and $\mathbf{G}_j(\mathbf{x})$ represents the j-th design constraint, such as stress component of an element for a given load case or the natural vibration frequency of a given mode .The total number of constraints may be very large. For large problems, it is not unusual to consider several thousand constraints. The objective

function, OBJ(x), is typically structural weight, but it can be exchanged with one of the structural responses. For example, one may desire to minimize dynamic displacement of a given degree of freedom for a specific load case, while satisfying all other design requirements and imposing an upper bound on structural weight.

EXAMPLE I - SIMPLY SUPPORTED BEAM

The example considered is a simply supported beam subject to a gravity load as well as an unbalanced rotating load as shown in Fig. 1. This is a simple example , yet it has all the necessary ingredients to demonstrate the capabilities of the design procedure outlined in this paper, including integration of static and dynamic design capabilities. Even though the loading is not symmetric, the structure and support conditions are symmetric with respect to the mid-plane A-A; thus only the right half is modeled using 15 QUAD4 elements. Symmetric and asymmetric boundary conditions are imposed to capture both symmetric and asymmetric responses. The right half model is divided into five sections of equal length and two independent design variables are associated with each section: uniform thickness and uniform non-structural mass. Consequently, the total number of design variables is ten; five for structural thicknesses and five for non-structural masses. The static load is a vertical 60 g gravity. Stresses are computed on both upper and lower surfaces at the centroid of each element. The initial design has uniform thickness of one inch and non-structural mass is equal to the structural mass distribution. The primary structural responses of the initial design are summarized in Table 1.

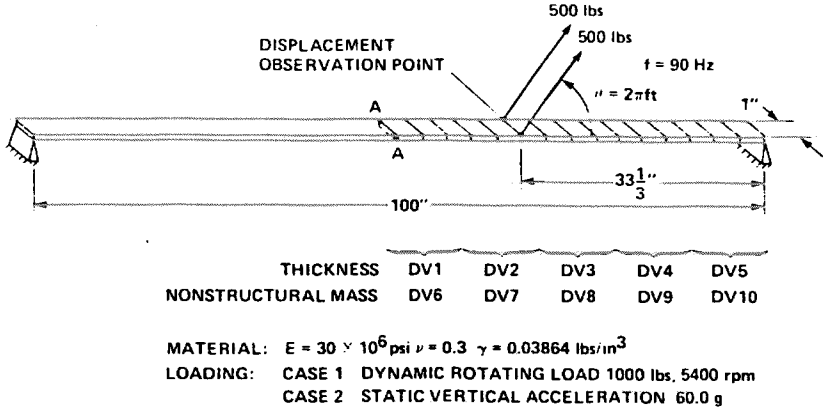

FIGURE 1 SIMPLY SUPPORTED BEAM

Problem I-a.

Minimize:	Total weight			
Subject to:	Stress	≤	30,000 psi	(all elements)
	U_s	≤	2.0 in	
	U_d	≤	1.5 in	

where U_s and U_d are static and dynamic vertical displacements at the observation point located at 33.3 inches from the right support. For this problem, natural frequencies were not constrained, although they were

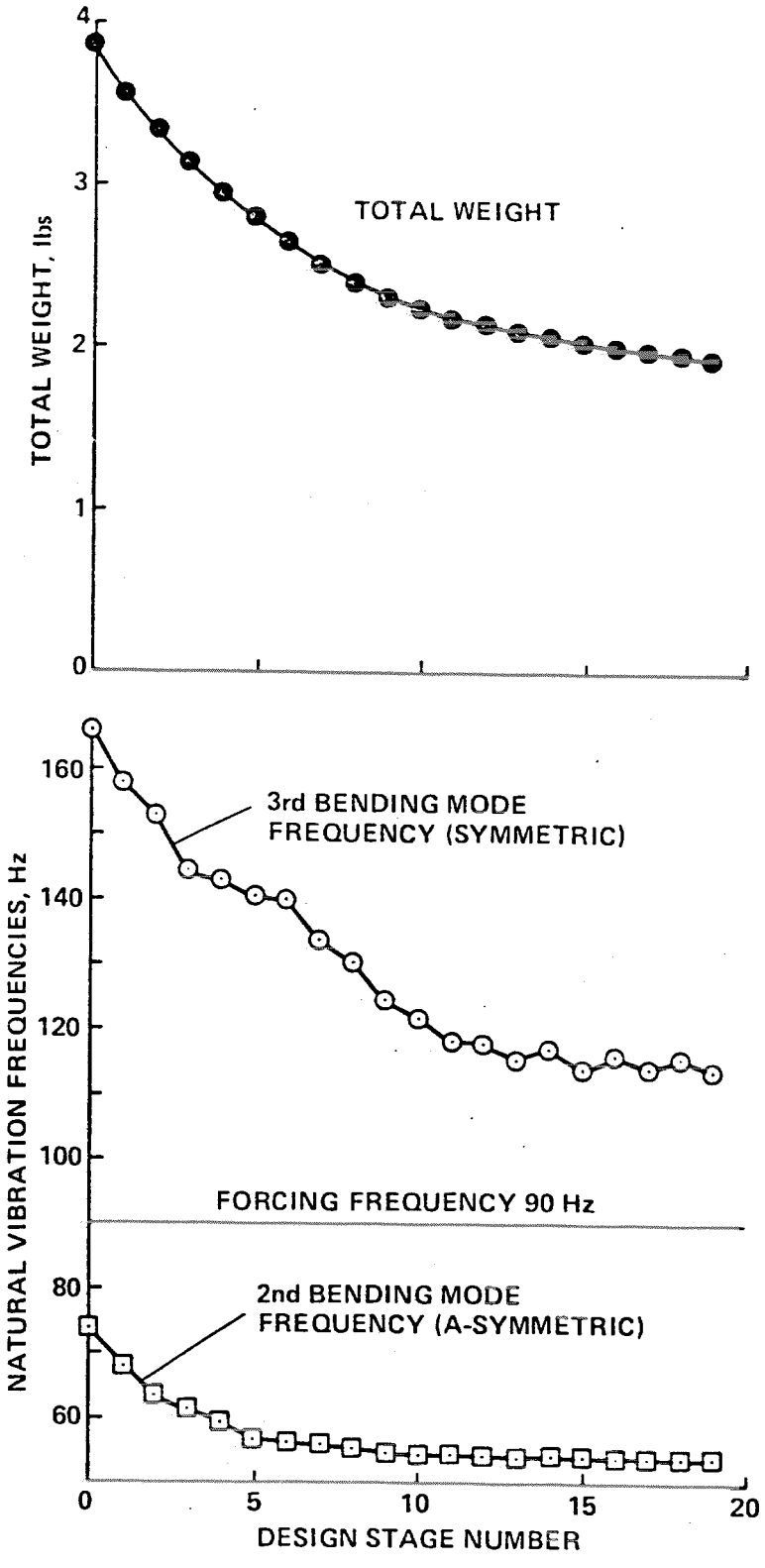

FIGURE 2 ITERATION HISTORY PROBLEM I-a

monitored every time a complete MSC/NASTRAN analysis was performed. The initial expectation was that natural frequency placement might be incidental to the constraints on dynamic response. The iteration history for this problem is presented in Fig. 2 and Table 2. The weight approached 1.65 pounds (half model) after 20 iterations, and the second and the third natural frequencies were adjusted such that the excitation frequency was almost equally distant from each of them. Note that the first mode is not affecting the dynamic responses since its frequency is very low compared to the forcing frequency. This case was run using relatively small move limits of 10%, i.e., each design variable cannot change its value more than 10% within a design iteration. This was done to avoid excessive oscillatory behavior of the optimization process. The oscillatory behavior is attributed in part to the fact that the bending stiffness is proportional to the cube of the plate thickness, thus the linear approximation used in this program tends to overscale the design. It was observed that the thicknesses of the two inboard sections tend to trade off thicknesses with each other, presenting a minor zig-zagging behavior. The final design shown in Fig. 3 exhibits an interesting non-structural mass distribution, indicating the desirable tuning mass location at the second section from the support.

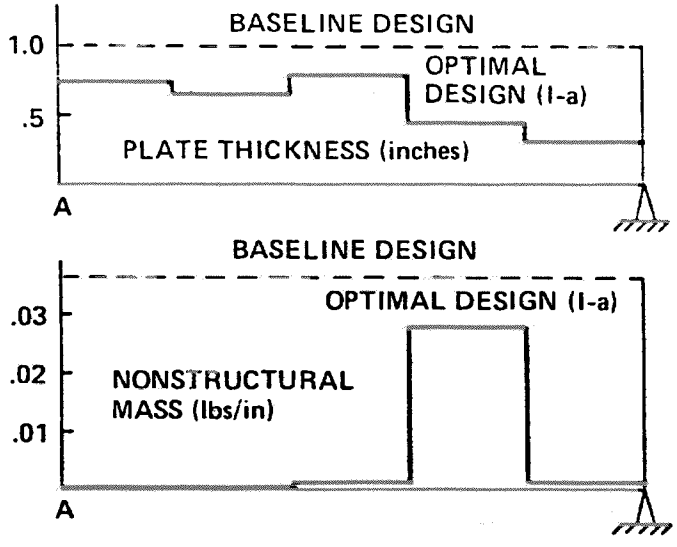

FIGURE 3 OPTIMAL MATERIAL DISTRIBUTION PROBLEM I-a

Problem I-b.

Minimize:	Ud (observed dynamic response)		
Subject to:	Total half model weight	$\leq$	3.0 lbs
	Stress	$\leq$	30.000 psi
	Us	$\leq$	2.0 in
	70 Hz $\leq f_2 \leq$ 75 Hz		
	150 Hz $\leq f_3 \leq$ 180 Hz		

where f_2 is the natural vibration frequency of the second bending mode (asymmetric) and f_3 is the frequency of the third bending mode (symmetric). Initially, this problem was tried without frequency constraints and the process failed to converge even with 10% move limits. The cause of this failure was

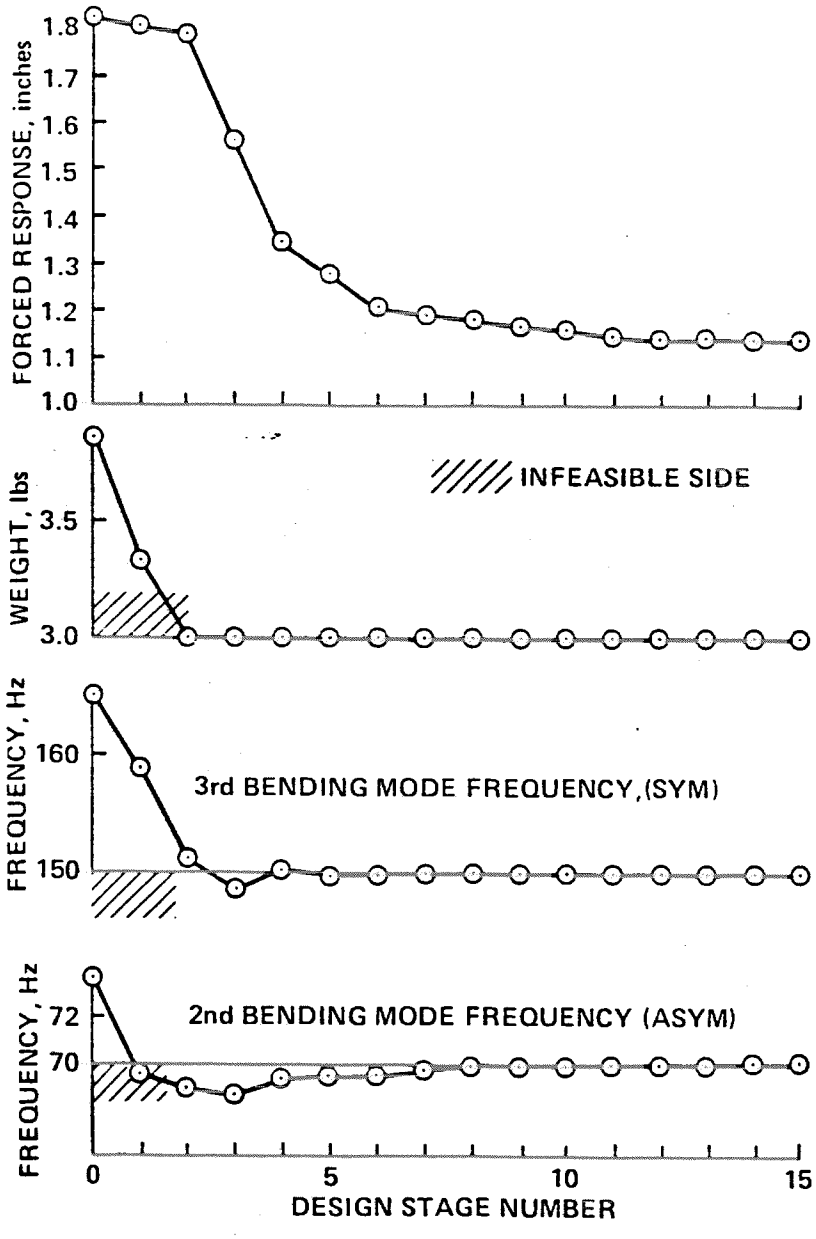

FIGURE 4 ITERATION HISTORY PROBLEM I-b

found to be the strong nonlinearity of the dynamic response when the third natural frequency approached the driving frequency. The optimizer was attempting to excite only one vibration mode and adjust that mode shape to have a node at the observation point. However, when the frequency of the third mode approached the driving frequency, the nonlinearity of the dynamic response with respect to design variables became very strong and required extremely small move limits, less than 1-2% as shown in Appendix A. Instead of reducing the move limits, frequency constraints were introduced to prohibit any of the natural frequencies from approaching the driving frequency as

TABLE 1 STRUCTURAL CHARACTERISTICS OF INITIAL & OPTIMAL DESIGNS-Problem I

		Initial Design	Optimal Design I-a	Optimal Design I-b
Total Weight	(lbs)	3.864	1.646	3.012
Static Disp.	(in)	1.908	2.042	1.094
Max. Stress	(psi	30840	30150	29270
Dynamic Disp.	(in)	1.827	1.490	1.137
Natural Freq.	(Hz)			
Mode 1 (symm)		18.4	17.9	24.3
2 (asymm)		73.6	52.9	70.0
3 (symm)		165.5	113.1	149.9
Design Variables				
1	(in)	1.0	0.86970	1.08620
2	(in)	1.0	0.77200	1.61190
3	(in)	1.0	0.92720	2.07640
4	(in)	1.0	0.52940	0.75730
5	(in)	1.0	0.37380	0.50920
6	(lbs/in^2)	0.03864	0.00032	0.00209
7	(lbs/in^2)	0.03864	0.00035	0.00261
8	(lbs/in^2)	0.03864	0.00149	0.01573
9	(lbs/in^2)	0.03864	0.02762	0.04584
10	(lbs/in^2)	0.03864	0.00055	0.00194

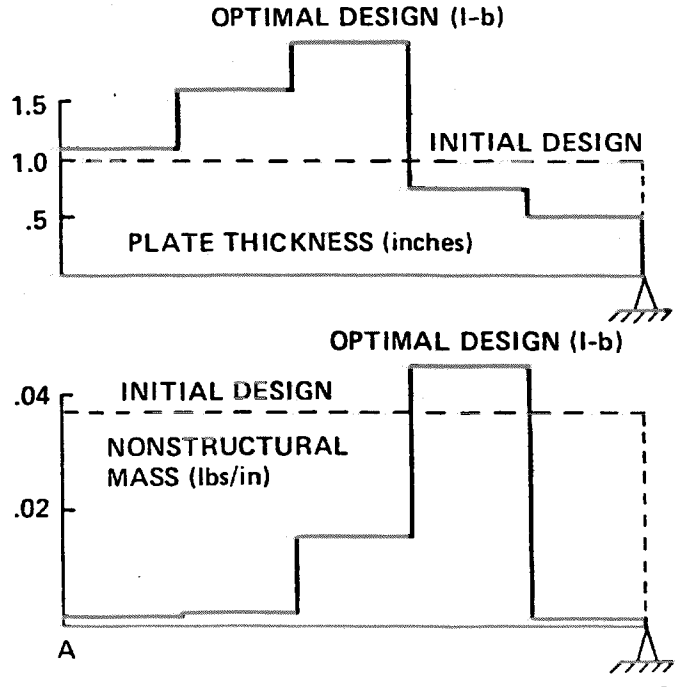

FIGURE 5 OPTIMAL MATERIAL DISTRIBUTION PROBLEM I-b

stated above. Iteration history and the final design are presented in Figs. 4 and 5. It was not possible to make the dynamic displacement less than 1.137 inches under the conditions stated above. It is important to know the influence of the imposed design conditions on the performance of the optimal design and the method presented here provides that critical information. If the frequency or weight requirements are relaxed, achievable dynamic displacement will be lower. It is possible to estimate such sensitivities by applying repeated design optimizations. To satisfy the frequency requirements, the final design retained more material compared to the previous case I-a.

EXAMPLE II - ENGINE SUPPORT STRUCTURE

The previous example demonstrated the validity of the techniques developed. To demonstrate the capability of these techniques, a design example of significant size and complexity was chosen. This example involves the vibration minimization of a engine support structure. It has the attributes required to demonstrate the features that were developed such as: static displacement/stress constraints as well as dynamic displacement minimization.

Only one half of the structure is shown in Fig. 6, since it is symmetric with respect to the Y-Z plane. The dimensions of the whole structure are approximately 300 in, 200 in and 200 in for the X,Y, and Z directions, respectively. The weight of the whole structure is about 230,000 lbs. It consists of four main components: Engine housing, Fig. 7; Subbase, Fig. 9; Engine shaft, shown in Fig. 6 as a line with dots; and lastly, the auxiliary equipment, which is not shown but is located in the cavity of the subbase adjacent to the engine. The auxiliary equipment is treated as a concentrated mass which is connected to the subbase via the RBE3 elements.

In this example, only the subbase was considered as a candidate for optimization. To minimize the analysis model size, the engine housing and rotors were modeled as dynamic superelements with component modes up to 240 Hz. The resulting analysis model consists of 991 grid points, 5000 free degrees of freedom and 1105 elements. The maximum number of active columns is 483 and the RMS value is 303.

The static loading on the structure consists of three gravity loads in the three orthogonal directions. The steady state dynamic loads originate from two different sources. One is due to the rotor mass unbalance and the other is due to the deformation of the auxiliary equipment structure by the rotating magnetic field. The location and magnitude of these loads are shown in Figs. 9 and 10. The two 10-lb loads represent the rotating mass unbalance while the other three loads represent the generator stator loads. This propulsion unit is a synchronous speed machine, therefore the force excitation occurs at the fundamental harmonic and its multiples. For this analysis a single excitation frequency of 120 Hz was used since the modal density is much greater at 120 Hz than at the fundamental harmonic, thereby making the 120 Hz a much more interesting frequency.

The whole structure is supported on four points (two are shown in Fig. 6; 3201 & 3204) when the structure is subjected to the steady state dynamic loads. The static gravity loads in reality represent shock loads so when these loads are applied additional supports become activated; i.e. snubbers. Hence,

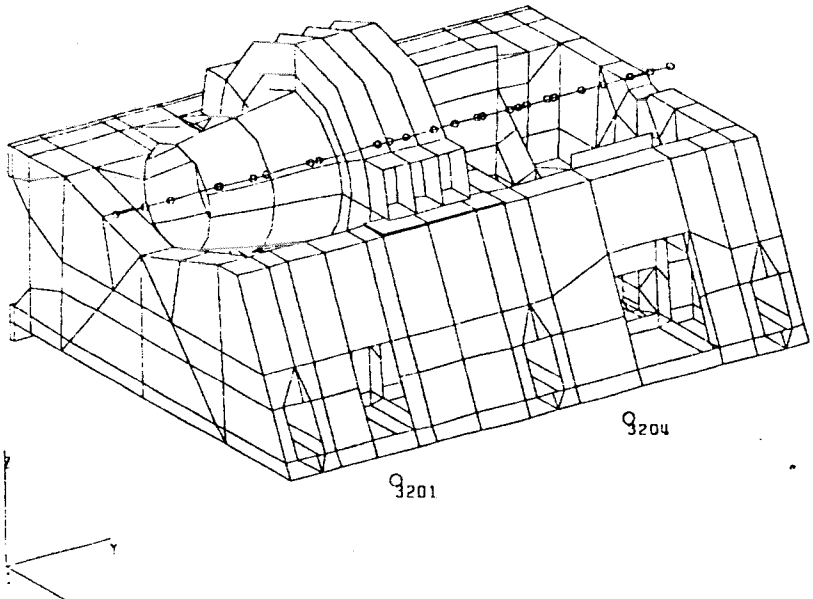

FIGURE 6 ENGINE SUPPORT STRUCTURE

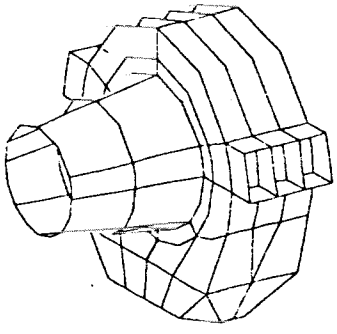

FIGURE 7 ENGINE HOUSING

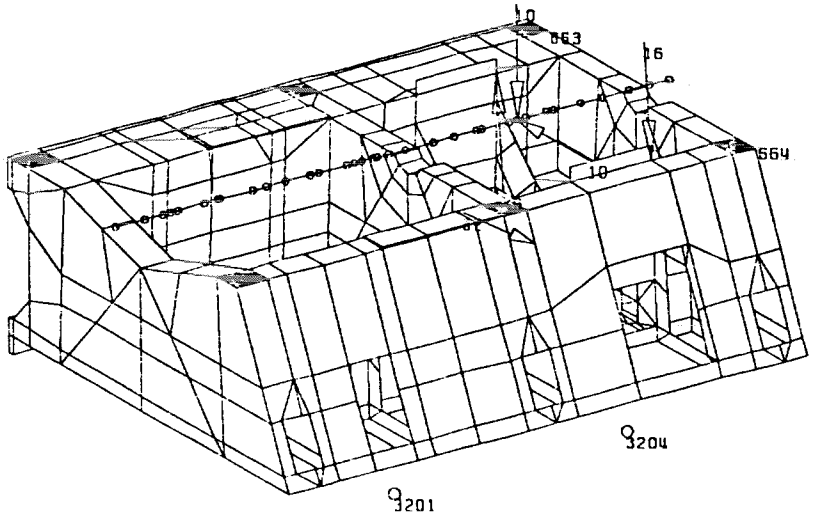

FIGURE 9 SUBBASE

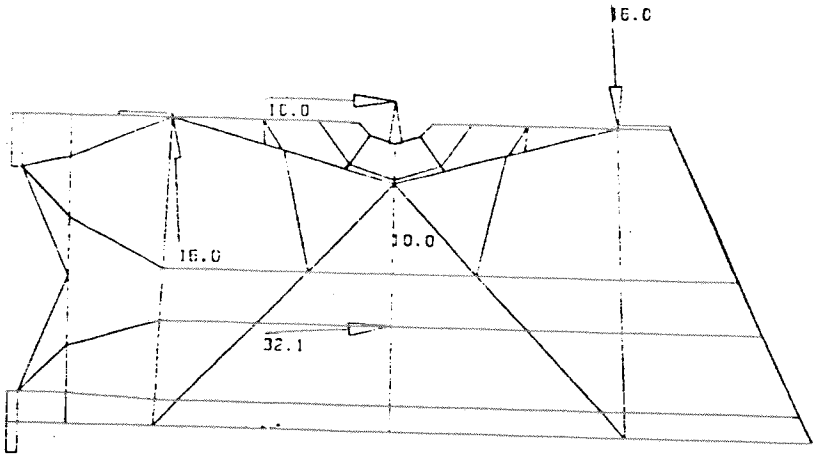

FIGURE 10 DYNAMIC LOADS

it is necessary to change boundary conditions depending on the load condition. In order to obtain the required static and dynamic responses for half model, four different boundary conditions were used. A total of 11 unique loads were applied and 4 additional loads were generated by combination of the other 11. This number of loads is due to the necessity of decomposing the actual loads into symmetric and asymmetric components.

The structure has a number of sources of damping. The overall structural damping factor was set to 0.03 which is found in similar structures. The oil-film bearings that support the rotor offer significant localized damping. Likewise, the mount system between the subbase and points 3201 and 3204 also provides localized damping.

The optimization objective is to minimize the dynamic forces and/or accelerations transmitted to the support points 3201 & 3204 in the three orthogonal directions. As noted previously, there are two dynamic force systems whose phase relationship is unknown. There are also a total of 6 support forces for each load case (i.e., 2 support points * 3 directions). To obtain a single quantity for the objective function, a square root of the sum of the squares of all support forces for both loads was selected as the objective function. Constraints were placed on the allowable stresses due to static loads and on the weight of the structure. The optimization problem can be summarized as,

Minimize:	RMS forces at two points for excitation at 120 Hz.	
Subject to:	Weight	$\leq$ 115,000 lbs
	Von-Mises Stress/static	$\leq$ 80,000 psi

There are 22 design variables in the problem. The design variables are the thicknesses of plate elements and "tuning" masses. There are 16 different thicknesses and 6 "tuning" masses that are allowed to vary. Minimum thickness is 0.375 in and the maximum is 4.0 in. Minimum "tuning" mass is 0

lb and there is no maximum limit since that constraint is incorporated in the constraint on the weight of the whole structure. There are 692 plate elements that are being designed and another 413 that are not designed but whose stresses have to be within the allowable values.

It is a well-known fact that strategically located mass can sometimes significantly reduce structural vibration. Since it is not known a priori where the optimal locations might be, six different locations, shown as dark rectangles in Fig. 9, were chosen for "tuning" mass placement. An initial mass of 300 lbs was placed at each location. Subsequently, the optimization process can increase the mass at those locations which have beneficial effect and reduce to zero, if necessary, the mass at locations that are ineffective.

Since in the previous example problems were encountered with the size of the move limits, two different sets of move limits were used to study their effect on the convergence and accuracy of the approximate analysis. The two sets of move limits on the normalized variables were

1. $0.90 \leq \quad T \quad \leq 1.10$
   $0.80 \leq \text{NSM} \leq 1.20$

2. $0.80 \leq \quad T \quad \leq 1.20$
   $0.70 \leq \text{NSM} \leq 1.30$

where T and NSM represent thickness and "tuning" masses, respectively. Based on previous experience, it was assumed that the non-linearities in the dynamic response associated with "tuning" masses would be smaller than that due to the plate thicknesses. Consequently, the move limits for NSM were made larger than the move limits for T's.

Nearly 20 iterations were performed in both cases. The CPU time for each iteration is shown in Table 2. It is clear that the optimization time for the approximate model is insignificant compared to the time required to perform the analysis and sensitivity calculations. Normal modes analysis was performed

TABLE 2 CPU TIME SUMMARY (CRAY-XMP/48 COMPUTER)

Operation		CPU Time (sec)
MSC/NASTRAN Analysis		297.0 (204)*
Constraint Sort		10.3
MSC/NASTRAN Sensitivity		346.5 (276)*
Approximate Optimization		1.5
	Total per iteration	655.3
Normal Modes	(Inv)	679
	(Lanczos)	175

* Solution times after the static loads were eliminated

only for the initial and final or "optimal" designs. In both cases only the modes in the range of 115 to 125 Hz were found. Incidentally, it is obvious that Lanczos method is vastly superior to the Inverse Power method of eigenvalue extraction. Early in the iteration process it was found that the static stresses were far below their allowable values. To reduce the computation time, the static loads were eliminated from the analysis, thereby saving 164 CPU sec per iteration.

The iteration history of the rms force for the two sets of move limits is shown in Fig. 11. Paradoxically, the higher move limits gave a superior and a more convergent solution. During the iteration process a comparison was made between the rms force values provided by the exact analysis and the approximate linearized analysis. When these values started to diverge, indicating a presence of strong non-linearity, the move limits were changed and a solution restarted from the last iteration where the values were still reasonably close. Table 3 shows the iteration history for the exact and approximate analysis. Divergence occurred at the 13th and 9th iterations for the two move limits. At these iterations the solution was continued, but the move limits were set to $0.95 \leq T \leq 1.05$ and $0.875 \leq NSM \leq 1.125$ for both problems. Five design variables were removed from the problem since their values did not change for a number of previous iterations. Removing those variables reduced the time to perform the sensitivity analysis.

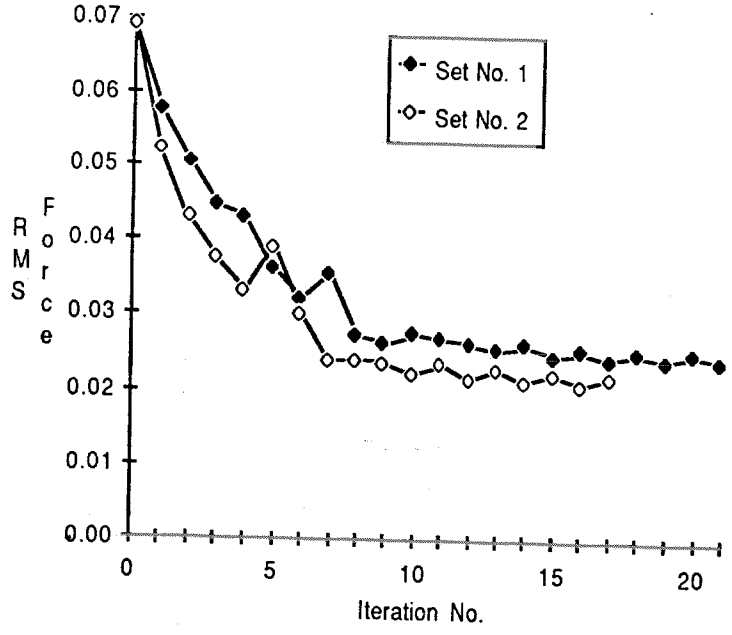

FIGURE 11 OPTIMIZATION HISTORY

The two solutions do "converge" even though the convergence is oscillatory. The exact and approximate analysis still differ between 10 and 20 percent, indicating a source of oscillatory behavior. The rms force value of

TABLE 3 RMS FORCE FOR TWO SETS OF MOVE LIMITS

Iteration	Set No. 1		Set No. 2	
	Exact	Approx	Exact	Approx
0	.0688	-	.0688	-
1	.0578	.0562	.0521	.0480
2	.0507	.0506	.0428	.0447
3	.0447	.0458	.0378	.0385
4	.0431	.0381	.0332	.0342
5	.0362	.0397	.0391	.0409
6	.0322	.0323	.0303	.0311
7	.0356	.0231	.0240	.0197
8	.0273	.0310	.0240	.0054
9	.0264	.0210	.0239	.0179
10	.0278	.0228	.0223	.0189
11	.0269	.0157	.0237	.0186
12	.0264	.0147	.0215	.0177
13	.0256*	.0245	.0231	.0182
14	.0263	.0235	.0211	.0175
15	.0250	.0232	.0223	.0181
16	.0256	.0228	.0209*	.0175
17	.0245	.0229	.0221	.0181
18	.0252	.0226	-	-
19	.0245	.0222	-	-
20	.0253	.0223	-	-
21	.0244	.0217	-	-

* Move limits changed to $0.95 \leq T \leq 1.05$
$0.875 \leq NSM \leq 1.125$
and five design variables were eliminated

.0209 obtained after the 16th iteration from the second set of move limits is considered as the optimum value. This value represents a reduction of .304 or -10.3 db from the original starting value. Table 4 presents the list of the starting and final values for all the design variables. It is interesting to note that the optimization process essentially removed four of the six "tuning" masses while significantly increasing the other two. Their locations are indicated in Fig. 9 as 663 and 664 and their respective values are 2877 and 2002 lbs.

Normal mode analysis was performed for the original and final design in the range of 115 to 125 Hz. This was done to understand the effect of the optimization process on the modes in the vicinity of the excitation frequency of 120 Hz. If an assumption is made that the response can be obtained from linear superposition of the modes in the neighborhood of the excitation frequency, then the reduction of the dynamic response can be studied by observing the impact on those modes. Participation factors, defined as $\emptyset^t_i F/k_i$, were calculated for each mode. $\emptyset_i$ is the mode shape, F is the spatial distribution of the load, and k_i is the generalized stiffness of each mode. The list of frequencies and participation factors is shown in Table 5. It is obvious

TABLE 4 OPTIMIZATION SUMMARY

Design Variable	Pid	Type	Initial Design	Final Design
1	50	T	0.375	0.393
2	52	T	0.375	0.375
3	53	T	0.375	0.375
4	55	T	0.500	0.375
5	57	T	0.375	0.375
6	80	T	0.375	0.375
7	83	T	0.375	0.443
8	84	T	0.500	0.375
9	88	T	0.375	0.375
10	89	T	0.500	0.815
11	100	T	0.500	0.375
12	101	T	0.500	0.375
13	151	T	0.750	0.795
14	152	T	1.500	0.375
15	155	T	2.000	0.764
16	158	T	1.500	0.619
17	661	NSM	300.	22.30
18	662	NSM	300.	21.01
19	663	NSM	300.	2877.47
20	664	NSM	300.	2002.08
21	665	NSM	300.	18.34
22	666	NSM	300.	15.36
RMS Force			0.0688	0.0209

that there has not been a significant shift in the number of modes or in their values for the range specified. The reduction in the response can be attributed to the change in the mode shapes as demonstrated by the reduction in the rms values of the participation factors. The total rms value of the final/initial is .328/.699 = .469. The physical response is equal to $\sum \emptyset_i \emptyset^t_i F/k_i$ (DAF_i), where (DAF) is the dynamic amplification factor that depends only on the ratio of the forcing to natural frequency. In the equation, the participation factor is multiplied by the mode shape $\emptyset_i$. It is very plausible, then, that a further reduction in the .469 factor will occur due to this multiplication, thereby explaining the ratio of the final to initial response. It is worth noting that this was achieved without ever explicitly dealing with mode shapes or their derivatives which can be very costly to obtain.

In the past an attempt would have been made to move the natural frequencies away from the frequency of excitation. It is evident that such an attempt would have failed because it is not possible to predict, with so many modes, which mode should be constrained to be above and which should be below the excitation frequency. The current approach avoids that difficulty by dealing directly with the response quantity.

TABLE 5 MODAL PARTICIPATION FACTORS FOR FREQUENCIES BETWEEN 115 AND 125 Hz

	Initial Design			Final Design		
SYMMETRIC		LOAD No.			LOAD No.	
Mode	Freq	1	2	Freq	1	2
44	116.91	3.33-1	1.09-2	115.25	7.66-2	3.87-3
45	118.16	8.52-2	5.65-3	116.52	8.27-2	1.40-2
46	121.67	5.34-1	2.61-3	118.90	9.94-3	4.89-3
47	123.89	2.03-1	3.89-3	121.70	7.30-2	1.87-3
48				122.56	2.65-1	5.52-4
		RMS = .667			RMS = .298	
ASYMMETRIC		LOAD No.			LOAD No.	
Mode	Freq	1	2	Freq	1	2
45	115.69	2.61-2	3.15-3	117.81	1.07-1	5.24-3
46	118.89	1.98-1	1.52-2	119.08	2.26-2	1.61-2
47	121.40	5.14-2	8.92-3	121.60	7.77-2	7.11-3
48	122.99	2.73-2	6.36-4	122.65	2.71-2	2.64-4
		RMS = .209			RMS = .138	
		Total RMS =.699			Total RMS =.328	

CONCLUDING REMARKS

Structural optimization capabilities obtained by integrating finite element structural analysis and nonlinear programming techniques through innovative use of approximation concepts, provide general and versatile tools to improve dynamic characteristics of structures. It is possible to consider a variety of design requirements simultaneously as long as adequate mathematical models and reliable analysis techniques are available for the corresponding responses. For example, static strength and stiffness requirements are taken into account while carrying out design modifications for improvement of dynamic performances. It has been demonstrated that the techniques described in this paper can be applied to actual design problems in a practical environment. Future research will be needed to obtain a more accurate approximation of dynamic response near the resonant condition. The difficulties associated with disjoint design space are yet to be conquered.

ACKNOWLEDGMENTS

The authors are grateful to Cray Research Inc. for providing the necessary computer time to obtain the solutions presented. This paper was previously published in "The Proceedings of the International Conference on Supercomputer Applications in the Automotive Industry", Zurich, Switzerland, October 1986, organized by Cray Research Inc., Editor: C. Marino.

REFERENCES

1. Done G. T. S. and Hughes A. D. (1976), Reducing Vibration by Structural Modification, Vertica, Vol. 1, pp.31-38.

2. Done G. T. S. and Rangacharyulu M. A. V. (1981), Use of Optimization in Helicopter Vibration Control by Structural Modification, J. of Sound and Vibration, Vol. 74, pp. 507-518.

3. Done G. T. S. (1981) Use of Optimization in Helicopter Vibration Control by Structural Modification, Northeast Region National Specialists' Meeting on Helicopter Vibration, Hartford, CT., 1981

4. Hanson H. W. and Calapodas N. J. (1980) Investigation of Vibration Reduction Through Structural Optimization, USAAVRADCOM TR-80-D-13.

5. Hanson H. W. and Calapodas N. J. (1980), Evaluation of the Practical Aspects of Vibration Reduction Using Structural Optimization Techniques, J. of American Helicopter Society, Vol. 25.

6. Sciarra J. J. (1974) Use of the Finite Element Damped Forced Response Strain Energy Distribution for Vibration Reduction, Boeing Vertol Company Report D21-10819-1 for U.S. Army Research Office, Durham, NC.

7. King S. P. (1983), The Modal Approach to Structural Modification, J. of American Helicopter Society, Vol. 28, pp. 30-36.

8. Wang B. P. Kitis L. Pilkey W. D. and Palazzolo A. B. (1982), Helicopter Vibration Reduction by Local Structural Modification, J. of American Helicopter Society, Vol. 27, pp. 43-47.

9. Kitis L. Pilkey W. D. and Wang B. P. (1983), Optimal Passive Frequency Response Control of Helicopters by Added Structures, AIAA Paper No.83-27976 backup document for a synoptic in AIAA J. Aircraft, same title.

10. Bartlett F. D. (1983), Flight Vibration Optimization via Conformal Mapping, J. of American Helicopter Society, Vol. 28, pp. 49-55.

11. Schmit L. A. and Miura H. (1976) Approximation Concepts for Efficient Structural Synthesis, NASA CR-2552.

12. Vanderplaats G. N. Miura H. and Chargin M. K. (1985), Large Scale Structural Synthesis, Int. J. of Finite Elements in Analysis and Design, Vol.1, pp. 117-130.

13. Vanderplaats G. N. (1973) CONMIN: A FORTRAN Program for Constrained Function Minimization - User's Manual, NASA TMX-62-282.

14. Johnson E. J. (1976), Disjoint Design Space in the Optimization of

Harmonically Excited Structures, AIAA J. Vol. 14, pp. 259-261.

15. Mills-Curran W. C. and Schmit L. A. (1983) Structural Optimization with Dynamic Behavior Constraints, AIAA Paper 83-0936-CP, Proc. 24th AIAA/ASME/ASCE/AHS Structures, Structural Dynamics and Materials Conf. Lake Tahoe, 1983.

APPENDIX A

When one of the natural frequencies approaches the excitation frequency as a result of design change, optimization procedure based on the first order Taylor series approximation often fails to converge unless extremely small move limits are imposed. For example, problem I-b, without frequency constraints, exhibited very poor convergence. In one iteration, the optimizer modified the design from A to B given in Table A-1. The objective was to minimize the dynamic displacement at the observation point (see Fig. 1). Based on the approximate model generated at design A, the optimizer reduced the displacement from 0.68 inches to 0.158 inches. However, when the new design was analyzed by MSC/NASTRAN in the next iteration, the dynamic displacement for design B was found to be 2.64 inches. Therefore, the change from design A to B may be acceptable based on the approximate model generated at design A, but it cannot be justified with regard to the responses obtained by exact analysis.

TABLE A-1 RESPONSE BETWEEN DESIGN-A AND DESIGN-B

	Design-A	Design-X_1	Design-X_2	Design-X_3	Design-X_4	Design-B
Plate Thickness (in)	1.10747	1.08733	1.06720	1.04706	1.02693	1.00679
	0.92003	0.90330	0.88657	0.86985	0.85312	0.83639
	1.14879	1.17432	1.19985	1.22537	1.25090	1.27643
	0.52868	0.51907	0.50946	0.49984	0.49023	0.48062
	0.37311	0.36633	0.35954	0.35276	0.34597	0.33919
Nonstructural Mass(lb/in^2)	0.00840	0.00848	0.00855	0.00863	0.00870	0.00878
	0.01016	0.01084	0.01151	0.01219	0.01286	0.01354
	0.02876	0.03071	0.03267	0.03462	0.03658	0.03854
	0.03969	0.04233	0.04498	0.04762	0.05027	0.05292
	0.01816	0.01937	0.02058	0.02180	0.02301	0.02422
Weight (lb)	2.6274	2.6823	2.7372	2.7922	2.8470	2.9002
Static Disp. (in)	-2.2726	-2.4190	-2.5794	-2.7553	-2.9480	-3.1572
Dynamic Disp (in) (real part)	-0.2795	-0.5490	-0.3756	-0.1072	+0.4389	+2.6444
Frequencies (Hz)						
2nd Bending	45.14	43.39	41.68	40.02	38.41	36.86
3rd Bending	110.71	106.71	102.85	99.13	95.53	92.04

In order to study the exact responses between designs A and B, four additional designs between designs A and B were generated as follows:

$$X_s = X_A + 0.2\ s\ (X_B - X_A) \quad s = 1,2,3 \text{ and } 4 \qquad \text{(A-1)}$$

Three key structural responses computed by MSC/NASTRAN for these designs are plotted in Fig. A-1. Both static displacement and the third mode natural frequency are nearly linear with respect to the design variable changes. However, the dynamic displacement was found to be very nonlinear as the third mode frequency approached the excitation frequency of 90 Hz. The dynamic displacements for these designs are plotted in Fig. A-2. The distances between two adjacent designs are equal in the design space, while the dynamic response changes significantly faster when the design approaches design B. At design B, the third vibration mode is excited and dominates the displacement shape.

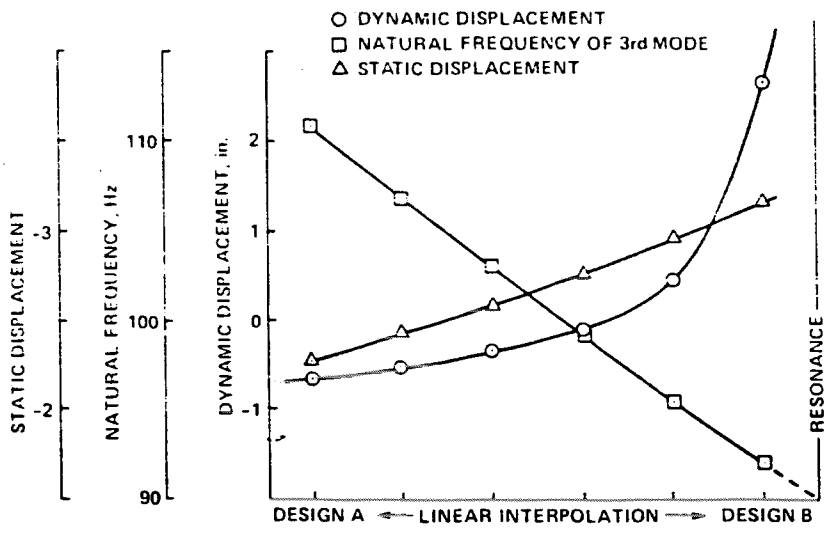

FIGURE A-1 STRUCTURAL RESPONSES

In some other problems it was necessary to use move limits of 0.5% or less, which resulted in discouragingly slow and difficult convergence characteristics. In order to alleviate difficulties associated with this nonlinearity, approximate models used for the dynamic displacement may have to be modified from the first order Taylor series expansion. One candidate for improved approximation may be in the form:

$$U_R+iU_I = \frac{C_R+iC_I + \sum_{k=1}^{K} (D_R+iD_I)\,(x_k-x_{ko})}{\prod_{p=1}^{P} \left[(1+ig)\frac{\bar{\omega}_p^2}{\Omega^2} - 1\right]} \qquad \text{(A-2)}$$

$$\text{where} \quad \bar{\omega}_p^2 = \omega_p^2 + \sum_{k=1}^{K} (x_k - x_{ko})\frac{\partial \omega_p^2}{\partial x_k} \qquad \text{(A-3)}$$

where (U_R+iU_I) is the approximation of the complex forced response vector, $w_{o1}, w_{o2}, \ldots, w_{oP}$ are the natural vibration angular frequencies near the excitation frequency, Ω, computed at the reference design X_o. x_k is the k-th design variable, (C_R+iC_I) is a constant complex vector and $(D_{Rk}+iD_{Ik})$ is a complex coefficient to be determined. The constants (C_R+iC_I) and $(D_{Rk}+iD_{Ik})$ can be computed from the complex displacement vector and its sensitivity vectors, obtained at the reference design X_o.

$$C_R+iC_I = (U_R+iU_I) \prod_{p=1}^{P} \left[(1+ig)\frac{\omega_p^2}{\Omega^2} - 1\right] \qquad \text{(A-4)}$$

$$D_R+iD_I = \frac{\partial(U_R+iU_I)}{\partial x_k} \sum_{p=1}^{P} [(1+ig)\frac{\omega_p^2}{\Omega^2} - 1]$$

$$- \frac{C_R+iC_I}{\Omega^2} \sum_{p=1}^{P} \frac{(1+ig)\ \partial\omega_p^2/\partial x_k}{(1+ig)\ \omega_p^2/\Omega^2 - 1} \qquad \text{(A-5)}$$

Since natural frequencies may be approximated reasonably well by the first order Taylor series expansion as shown in Eq. (A-3), the approximate form given in Eq. (A-2) is expected to follow the nonlinearities pointed out above. Sensitivity of the magnitude of the j-th displacement component, $(U_{Rj}^2 + U_{Ij}^2)^{1/2}$, can also be computed by chain rule differentiation.

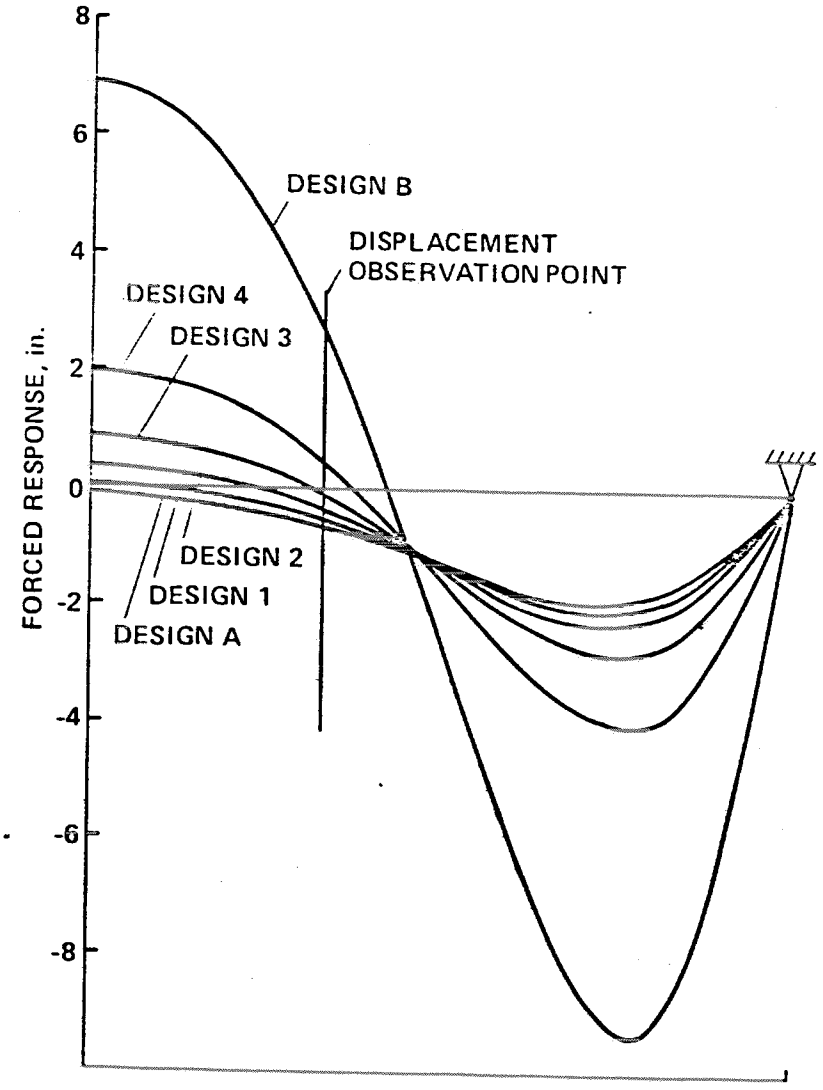

FIGURE A-2 DYNAMIC FORCED RESPONSES FOR SIX DESIGNS

If such approximations are not used, it is necessary to use proper move limits to avoid convergence difficulties. When only one mode is dominant, Eq. (A-2) has only one term in the denominator. For this case, the error caused by the first order Taylor series approximation applied to the dynamic displacement may be estimated analytically in terms of natural frequency perturbations. The results of this analysis are summarized in Fig. A-3. In this figure, the move limits imposed on the design variables are not explicitly available. Instead, the ratio of the natural frequency of the current design to the excitation frequency (w/Ω), perturbation of natural frequency caused by design perturbation ($\Delta w/\Omega$), and the expected amount of error for the dynamic displacement, delta, are presented. For example, if the excitation frequency is 10.8 Hz and the natural frequency is 9.0 Hz, the frequency ratio (w/Ω) is 0.8. To keep the error associated with the first order Taylor series approximation less than 15%, it is necessary to limit the design changes so that the natural frequency of that mode does not change more than 8%.

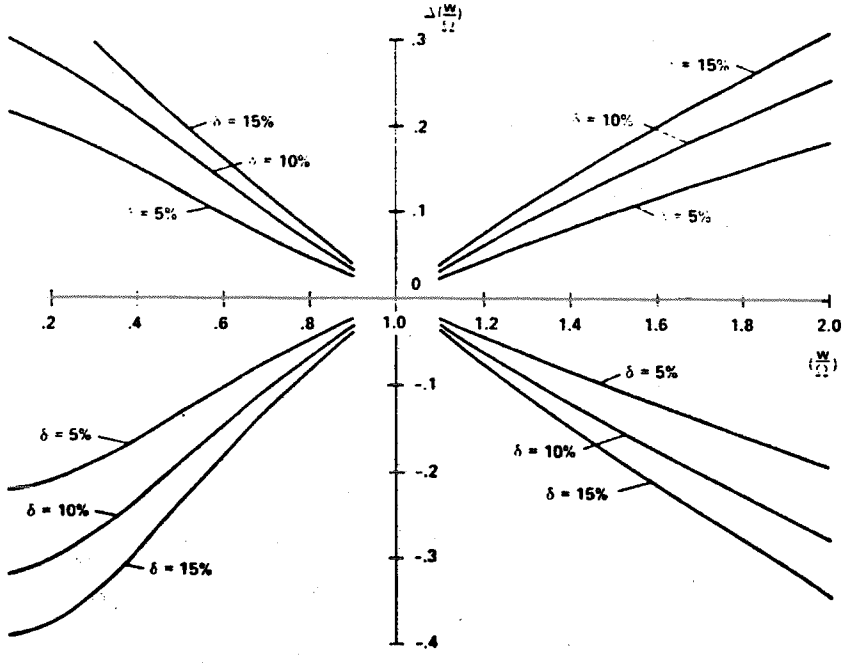

FIGURE A-3 ERROR OF LINEAR APPROXIMATIONS OF DYNAMIC RESPONSES